Theoretical calculations of dielectronic recombination in crossed electric and magnetic fields

D. C. Griffin
Department of Physics, Rollins College, Winter Park, Florida 32789

F. Robicheaux and M. S. Pindzola
Department of Physics, Auburn University, Auburn, Alabama 36849

(Received 14 October 1997)

Recently, Robicheaux and Pindzola [Phys. Rev. Lett. **79**, 2237 (1997)] reported on model calculations of dielectronic recombination (DR) in the presence of crossed electric and magnetic fields. They showed that the enhancement of the DR by an electric field may be increased further when a magnetic field perpendicular to the electric field is present in the collision region. In this paper, we describe the results of distorted-wave calculations of dielectronic recombination in the presence of crossed electric and magnetic fields for Li-like C^{3+} and Si^{11+}. Two sets of calculations are performed and compared. The first is based on a full intermediate-coupling (IC) calculation, while the second is based on a much simpler configuration-average (CA) approximation. Both sets of calculations predict substantial added enhancement of DR due to the magnetic field. However, the CA approximation overestimates the field-enhanced DR as compared to both the IC calculations and previous measurements of total recombination. Comparisons of our IC results with total recombination measurements are not possible because the IC Hamiltonian matrices are too large for the high values of n included in these experiments; however, in anticipation of possible high-resolution experimental studies of partial DR in fields, we report on an IC calculation of the crossed-fields enhancement of DR as a function of electric-field strength for $n=24$ in Si^{11+}. [S1050-2947(98)08904-5]

PACS number(s): 34.80.Lx

I. INTRODUCTION

Extensive experimental and theoretical studies of dielectronic recombination (DR) in the presence of external fields have been performed. Quite early, Burgess and Summers [1] suggested that the redistribution of angular momentum during collisions in a plasma could enhance DR and Jacobs and co-workers [2,3] predicted that plasma microfields would strongly enhance DR through such a redistribution of highly excited ℓ states. Huber and Bottcher [4] also pointed out that, in very strong magnetic fields, the diamagnetic term can also cause mixing of ℓ states. Since that time, there have been a number of calculations of DR in the presence of electric fields using a configuration-average distorted-wave approximation [5–7] and an intermediate-coupling, distorted-wave approximation [8–11]. There has also been a variety of measurements of DR in fields. The experiments at Oak Ridge National Laboratory on Na-like ions [12], Li-like ions [13], Be-like ions [14], and B-like ions [15] all suggested an enhancement of DR by the space-charge-produced electric field in the collision region, and the measurements at the Joint Institute for Laboratory Astrophysics on Mg^+ [16], provided the first experimental confirmation of the enhancement of DR as a function of the electric field in the collision region. More recently, DR measurements in the presence of small electric fields were made for a number of Li-like ions using a merged-beams apparatus at Aarhus [17,18] and measurements of DR in C^{3+} in a well-determined electric field were performed at Harvard [19,20].

In a number of the systems studied, the predicted enhancement from theoretical calculations was within the uncertainty of the experimental measurements. However, there are several examples where the experimental measurements were above those predicted from theory. In particular, the measurements by Dittner *et al.* [13] on Li-like ions were well above the theoretical calculations [8] for all reasonable electric field strengths. In addition, the measurements of Savin *et al.* [20] were above the theoretical calculations [6,8] but, within their large experimental uncertainties, agree with Griffin, Pindzola, and Bottcher [8].

More recently, an experiment was completed at the heavy-ion storage ring (CRYRING) at Stockholm University [21], in which the DR rate coefficient for Si^{11+} was measured and compared to theoretical calculations of electric-field-enhanced DR. The agreement between theory and experiment was excellent for the zero-field measurements, but the experimental values of the integrated rate coefficient as a function of electric field were above those determined from the theoretical calculations. As in all comparisons between experimental measurements and theoretical calculations of DR, there are a number of factors that could cause such differences, one of the most important of which is the uncertainty with respect to field ionization. However, there is sufficient evidence now to indicate that there may be additional enhancement of DR in these experimental measurements, beyond that due to electric-field mixing.

In response to this, Robicheaux and Pindzola [22] performed model calculations of dielectronic recombination in the presence of crossed electric and magnetic fields. Such crossed fields exist within the collision region in these experiments. The probability of recombination into doubly excited states (the reverse of autoionization) falls off rapidly with the angular momentum of the Rydberg states. Thus, an

electric field enhances DR by mixing states with different angular momenta and, thereby, opening up many more recombination channels. However, in the presence of an electric field alone, M is a good quantum number and the recombination probability falls off rapidly with the magnetic quantum number [8]. In the presence of a magnetic field alone or a magnetic field parallel to the electric field, M remains a good quantum number. However, when the magnetic field has a component that is perpendicular to the electric field, states with different magnetic quantum numbers are mixed; this will open up still more recombination channels and should further enhance DR. Indeed, the calculations of Robicheaux and Pindzola [22] indicate that there is additional enhancement caused by magnetic mixing and that it might be of sufficient size to account for the apparent discrepancies between experiment and theory. Recently, LaGattuta [23] also performed calculations of DR in Mg^+ in crossed electric and magnetic fields using his configuration-average DR program. He found substantial enhancement of the DR rate coefficient in support of the prediction of Robicheaux and Pindzola [22].

The intent of the present study is to follow up on the model calculations of Robicheaux and Pindzola [22] by performing distorted-wave calculations of DR in the presence of crossed electric and magnetic fields for C^{3+} and Si^{11+}. Two approaches have been employed. One is based on a full intermediate-coupling (IC), distorted-wave calculations of DR. However, these calculations are limited to intermediate values of the principal quantum number by the enormous size of the Hamiltonian matrices that are involved. For that reason, we have also performed a series of field-mixed calculations of DR based on a much simpler configuration-average (CA), distorted-wave approximation.

The remainder of this paper is organized as follows. In the next section, we give a brief description of the theoretical methods employed in these calculations. In Sec. III, we compare our IC and CA calculations of DR as a function of n with each other and our CA calculations of total DR with prior experiments; and, in anticipation of future high-resolution partial DR measurements, we present an IC calculation of partial DR for the resonances associated with $n=24$ in Si^{11+}. In Sec. IV, we summarize our results and suggest some theoretical and computational methods for further study.

II. THEORETICAL METHODS

The theoretical methods employed to perform IC calculations of DR in electric fields, as implemented in the program DRFEUD, is described in some detail in Griffin, Pindzola, and Bottcher [8]. Here we focus on the equations describing the Stark and Zeeman matrix elements associated with doubly excited Rydberg states in the presence of crossed electric and magnetic fields. We first assume that the electric field is in the z direction and the magnetic field is in the x direction, and consider doubly excited Rydberg states consisting of two singly occupied subshells in jK coupling. Then the Stark matrix element is given by

$$\begin{aligned}
&\langle n_j \ell_j j_j n \ell K J M | -\vec{E}\cdot\vec{r} | n_j \ell_j j_j' n' \ell' K' J' M' \rangle \\
&= E\,\delta_{M,M'}\delta_{j_j,j_j'}(-1)^{J+J'+j_j+2K+\ell'+(3/2)} \\
&\times \sqrt{(2J+1)(2J'+1)(2K+1)(2K'+1)} \\
&\times (-1)^M \begin{pmatrix} J & 1 & J' \\ -M & 0 & M' \end{pmatrix} \begin{Bmatrix} j_j & \ell & K \\ 1 & K' & \ell' \end{Bmatrix} \\
&\times \begin{Bmatrix} K & \frac{1}{2} & J \\ J' & 1 & K' \end{Bmatrix} \langle \ell || P^{(1)} || \ell' \rangle, \qquad (1)
\end{aligned}$$

where n_j, ℓ_j, and j_j are the principal, orbital angular momentum, and total angular momentum quantum numbers for the first excited electron, respectively; n and ℓ are the principal and orbital angular momentum quantum numbers of the Rydberg electron, respectively; and P is the dipole operator. The matrix elements for the paramagnetic term can be broken up into two parts:

$$\begin{aligned}
&\langle n_j \ell_j j_j n \ell K J M | -\vec{\mu}\cdot\vec{B} | n_j \ell_j j_j' n' \ell' K' J' M' \rangle \\
&= \langle n_j \ell_j j_j n \ell K J M | \mu_0 \vec{J}\cdot\vec{B} | n_j \ell_j j_j' n' \ell' K' J' M' \rangle \\
&+ \langle n_j \ell_j j_j n \ell K J M | \mu_0 \vec{S}\cdot\vec{B} | n_j \ell_j j_j' n' \ell' K' J' M' \rangle, \qquad (2)
\end{aligned}$$

where we have assumed that the g factor for the electron spin is equal to 2, and μ_0 is the Bohr magneton. The first term is given by the expression

$$\begin{aligned}
&\langle n_j \ell_j j_j n \ell K J M | \mu_0 \vec{J}\cdot\vec{B} | n_j \ell_j j_j' n' \ell' K' J' M' \rangle \\
&= \mu_0 B\,\delta_{n,n'}\delta_{\ell,\ell'}\delta_{j_j,j_j'}\delta_{K,K'}\delta_{J,J'}\tfrac{1}{2} \\
&\times [\sqrt{(J-M)(J+M+1)}\,\delta_{M',M+1} \\
&+ \sqrt{(J+M)(J-M+1)}\,\delta_{M',M-1}], \qquad (3)
\end{aligned}$$

while the second term is given by

$$\langle n_j \ell_j j_j n \ell K J M | \mu_0 \vec{S} \cdot \vec{B} | n_j \ell_j j_j' n' \ell' K' J' M' \rangle$$
$$= \mu_0 B \delta_{n,n'} \delta_{\ell,\ell'} (-1)^{3J+J'-j_j-j_j'+1} \sqrt{\frac{(2J+1)(2J'+1)(2j_j+1)(2j_j'+1)(2K+1)(2K'+1)}{2}}$$
$$\times \left[(-1)^M \begin{pmatrix} J & 1 & J' \\ -M & 1 & M' \end{pmatrix} \delta_{M',M-1} + (-1)^{M'} \begin{pmatrix} J & 1 & J' \\ -M & -1 & M' \end{pmatrix} \delta_{M',M+1} \right]$$
$$\times \sum_{L,S} \left[(-1)^{L+S} (2L+1)(2S+1) \sqrt{S(S+1)(2S+1)} \begin{Bmatrix} L & \frac{1}{2} & K \\ \frac{1}{2} & J & S \end{Bmatrix} \right.$$
$$\left. \times \begin{Bmatrix} L & \frac{1}{2} & K' \\ \frac{1}{2} & J' & S \end{Bmatrix} \begin{Bmatrix} L & S & J' \\ 1 & J & S \end{Bmatrix} \begin{Bmatrix} \ell & \ell_j & L \\ \frac{1}{2} & K & j_j \end{Bmatrix} \begin{Bmatrix} \ell & \ell_j & L \\ \frac{1}{2} & K' & j_j' \end{Bmatrix} \right]. \quad (4)$$

We notice the electric field mixes Rydberg states between $n\ell$ subshells that differ by one in ℓ, but the Stark matrix elements are diagonal in j_j and M. The electric field can also mix states of different values of n; however, for the electric-field strengths and the range of n values included in these calculations, the effects of n mixing should be very small.

The paramagnetic term mixes Rydberg states within a given $n\ell$ subshell that differ by one in M. We also notice that when the magnetic field is included in the Hamiltonian, j_j is no longer a good quantum number. We have found, however, that the effect of magnetic mixing between states of different values of j_j is small; at sufficiently high values of n, this makes it possible to diagonalize the Hamiltonian separately for different values of j_j. In addition, one can also include the diamagnetic term within the Hamiltonian matrix, and it will mix Rydberg states that differ by two in ℓ. This term was included by LaGattuta [23] in his CA calculation for Mg^+; however, for the magnetic fields considered here, the diamagnetic term would make a negligible contribution to field enhancement.

Thus, for the lower values of n, we assume that the only good quantum numbers are n_j, ℓ_j, and n and the diagonalization yields eigenvectors of the form

$$|n_j \ell_j n \gamma\rangle = \sum_{j_j,\ell,K,J,M} Y^{n_j \ell_j n \gamma}_{j_j \ell K J M} |n_j \ell_j j_j n \ell K J M\rangle; \quad (5)$$

while for higher values of n, where j_j is assumed to be a good quantum number, this becomes

$$|n_j \ell_j j_j n \gamma\rangle = \sum_{\ell,K,J,M} Y^{n_j \ell_j j_j n \gamma}_{K J M} |n_j \ell_j j_j n \ell K J M\rangle; \quad (6)$$

and where γ is a serial number used to completely specify an eigenvector.

Now we could have just as well assumed that the electric field is in the x direction and the magnetic field is in the z direction. We have also derived the expressions for the Stark and magnetic matrix elements for this case. Calculations performed with both sets of field directions allowed for a useful internal check of the programming of this problem.

Except for the added magnetic matrix elements that must be determined, the calculation of DR in crossed electric and magnetic fields is similar to our early calculations of DR in electric fields, and a description of the calculation of the electric-field-mixed autoionizing and radiative rates is given in Griffin, Pindzola, and Bottcher [8]. The only difference in the equations for the autoionizing and radiative rates for the case of crossed electric and magnetic fields arises from the sum over M in the equations for the eigenvectors. Once the field-mixed autoionizing and radiative rates are determined, we again use the independent-processes approximation to calculate the contribution to the energy-averaged DR cross section from resonance j using the equation

$$\sigma_j = \frac{\pi^2}{\Delta\epsilon G_I k_\epsilon^2} \frac{\sum_i A_a(j \to i) \Sigma_f A_r(j \to f)}{\sum_k A_a(j \to k) + \Sigma_f A_r(j \to f)}, \quad (7)$$

where $\Delta\epsilon$ is an energy bin width larger than the largest resonance width, G_I is the total statistical weight of the initial configuration, k_ϵ is the linear momentum of the continuum electron, $A_r(j \to f)$ is the radiative rate from a particular doubly excited state j to all states of a lower level f, and $A_a(j \to k)$ is the autoionizing rate from a particular doubly excited state j of the $(N+1)$-electron ion to all states of the level k of the N-electron ion. The sum over i in this equation represents a sum only over the levels of the initial ion configuration, while the sum over k represents a sum over all lower levels of the N-electron ion. When not comparing to experimental measurements, it is convenient to present the results of calculations in terms of the quantity $\sigma\Delta\epsilon$, since it is independent of any choice of the energy bin width.

We have modified the program DRFEUD to calcuate DR in the presence of crossed electric and magnetic fields in either of the two orientations of the fields discussed above. However, there are some limitations on the use of this code. The fact that M is no longer a good quantum number leads to significant computational problems. First of all, the Hamiltonian matrix becomes extremely large and has many near degeneracies. Secondly, we must determine all the eigenvalues and eigenvectors in order to calculate the required radiative and autoionizing rates.

For the dielectronic recombination associated with the $2s \rightarrow 2p$ excitation in the Li-like ions considered here, there are a total of $12n^2$ states for the doubly excited Rydberg configurations with a given value of n. For $n=20$, this requires us to diagonalize a 4800×4800 matrix; by $n=30$ the matrix has grown to $10\,800 \times 10\,800$, and diagonalizing such a matrix is impractical. By assuming that j_j is a good quantum number, we can reduce the problem so that for each value of n, we must diagonalize the $j_j=\frac{1}{2}$ matrix of size $4n^2$ and the $j_j=\frac{3}{2}$ matrix of size $8n^2$. For $n=20$, the $j_j=\frac{3}{2}$ matrix is 3200×3200, while at $n=30$, it has grown to 7200×7200. The upper limit of $n=30$ that we employ was then set by available computer memory. However, as we shall see, in the measurements of total DR performed to date on these ions, the upper limit on n before field ionization occurs is well above 30.

For these reasons, we also tried a second approach to this problem that is based on the CA approximation for DR. Some of our earlier work on DR employed the CA program DRACULA [24], and we have now modified that program to carry out approximate crossed electric and magnetic field-mixed calculations of DR. The zero-field wave functions $|n\ell m\rangle$ and energy levels $\varepsilon_{n\ell}$ are calculated using the configuration-average Hartree-Fock equations with the core electrons frozen. The total autoionization rate $A_a(n\ell)$ and the total radiative decay rate $A_r(n\ell)$ for the $n\ell m$ Rydberg state are calculated in a configuration average. The configuration-average orbitals are used to generate the $n^2 \times n^2$ Hamiltonian matrix

$$H^n_{\ell m,\ell' m'} = \varepsilon_{n\ell}\delta_{\ell\ell'}\delta_{mm'} + \langle n\ell m| -Ez + \mu_0 B L_x |n\ell' m'\rangle. \tag{8}$$

This real, symmetric matrix is diagonalized using standard programs to give the eigenstates j. The eigenvectors $Y^n_{\ell m,j}$ are used to construct the total autoionization and radiative rates from

$$A_a(nj) = \sum_{\ell m} A_a(n\ell)(Y^n_{\ell m,j})^2, \tag{9}$$

$$A_r(nj) = \sum_{\ell m} A_r(n\ell)(Y^n_{\ell m,j})^2, \tag{10}$$

which are used in Eq. (7) to calculate the contribution to the energy-averaged DR cross section from resonance j.

Of course, the great advantage of the CA approximation is that one must only diagonalize a $n^2 \times n^2$ matrix for each value of n, which makes it practical to include Rydberg states up to values of n corresponding to available experimental measurements. The disadavantage of the method is that it tends to overestimate the effects of field mixing, especially for lower values of n and lower field strengths.

III. RESULTS OF CALCULATIONS

A. Comparison of intermediate-coupling and configuration-average calculations

We will begin by considering the results of our IC calculations on C^{3+} and Si^{11+}. In Fig. 1, we show our results for $\sigma\Delta\epsilon$ (with the energy bin width in Hartree atomic units) for C^{3+} from $n=8$ to $n=30$ for no fields, an electric field of 12 V/cm and no magnetic field, and finally an electric field of 12 V/cm and a magnetic field of 24 G. These field strengths were chosen so as to match the fields in the experimental measurements of Savin *et al.* [20]. The diagonalizations were carried out on all states of a given principle quantum number up to $n=20$ and then separately for each of the two values of j_j from $n=22$ to 30.

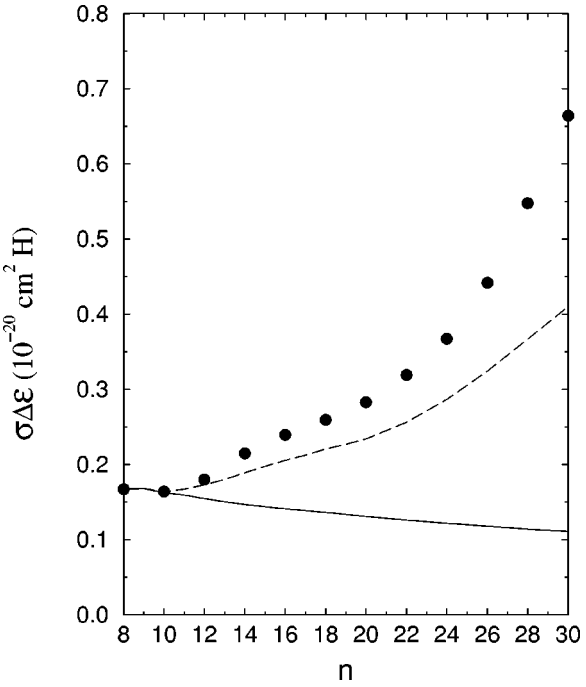

FIG. 1. The energy-averaged dielectronic recombination cross section times the energy-bin width as a function of n for C^{3+} from an IC calculation. Solid curve, no fields; dashed curve, an electric field of 12 V/cm, but no magnetic field; solid circles, an electric field of 12 V/cm and a magnetic field of 24 G.

As can be seen from this figure, the added enhancement of DR provided by the crossed magnetic field is small below $n=20$, but increases rapidly as a function of n. By $n=30$, this additional enhancement is nearly equal to that provided by the electric field alone, and is even larger than that predicted from the model calculations of Robicheaux and Pindzola [22]. It is not clear from these results at what value of n the cross section will peak and begin to decrease. However, these calculations in the presence of crossed electric and magnetic fields required over 430 megabytes of main memory and took 5 h on a Cray C90 computer; to carry out these calculations to say $n=44$, which was the estimated maximum value of n in the experiment of Savin *et al.* [20], would have required two gigabytes of main memory and many more hours of computer time.

In Fig. 2, we again present our IC results for C^{3+} for the same values of n, but now with an electric field alone of 30 V/cm and crossed electric and magnetic fields of 30 V/cm and 180 G, respectively. These field strengths were chosen to be comparable to those present in the experimental measurements of Dittner *et al.* [13]. With these fields, the overall enhancement is not only larger in magnitude, but the added enhancement from the magnetic field is now larger than that due to the electric field alone.

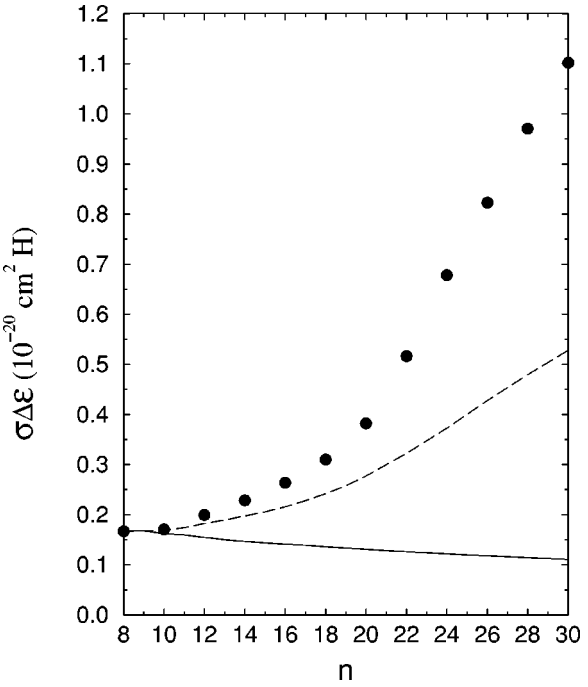

FIG. 2. The energy-averaged dielectronic recombination cross section times the energy-bin width as a function of n for C^{3+} from an IC calculation. Solid curve, no fields; dashed curve, an electric field of 30 V/cm, but no magnetic field; solid circles, an electric field of 30 V/cm and a magnetic field of 180 G.

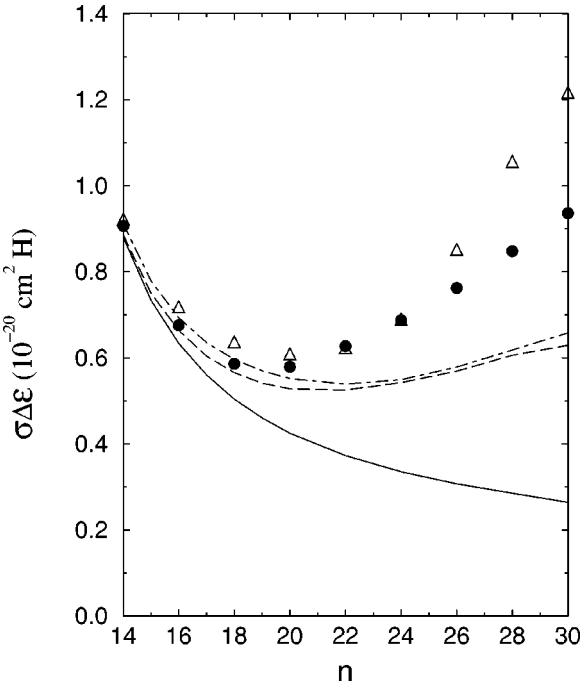

FIG. 3. The energy-averaged dielectronic recombination cross section times the energy-bin width as a function of n for Si^{11+} from an IC calculation. Solid curve, no fields; dashed curve, an electric field of 100 V/cm, no magnetic field, and the energy-level structure for high angular momentum states determined from extrapolation; dashed-dot curve, an electric field of 100 V/cm, no magnetic field, and the energy-level structure for high angular momentum states calculated using hydrogenic wave functions and perturbation theory; solid circles, an electric field of 100 V/cm, a magnetic field of 300 G, and the energy-level structure for high angular momentum states determined from extrapolation; open triangles, an electric field of 100 V/cm, a magnetic field of 300 G, and the energy-level structure for high angular momentum states calculated using hydrogenic wave functions and perturbation theory.

In Fig. 3, we present our IC results for $\sigma\Delta\epsilon$ for Si^{11+} from $n=14$ to $n=30$, for no fields, an electric field of 100 V/cm and no magnetic field, and finally an electric field of 100 V/cm and a magnetic field of 300 G. The magnetic field we employed is equal to the longitudinal magnetic field in the cooler of the CRYRING at the University of Stockholm where the experiment of Bartsch *et al.* [21] was performed, and the electric field is in the middle of the range of those fields employed in their experiment.

For the electric field alone and the crossed electric and magnetic fields, we show the results of two separate calculations. This is done to demonstrate the sensitivity of the crossed-fields calculations to the details of the atomic structure for high-ℓ Rydberg states. For the present calculations, in addition to the spin-orbit parameter of the $2p$ electron, there are only two parameters of much importance to the energy of a particular level belonging to a high-ℓ Rydberg state: they are the configuration-average quantum defect of the $2pn\ell$ configuration and the quadrupole Slater parameter $F^2(2pn\ell)$, the latter of which only affects the levels associated with $j_j=3/2$. The exchange parameters and the spin-orbit parameter of the outer electron are very small for high values of ℓ. To calculate the structure of the Rydberg states for relatively low ℓ values (in the case of Si^{11+}, $\ell\leqslant 7$) we employ parameters calculated using the wave function program developed by Cowan [25]. The wave functions are solutions to the Hartree-Fock equations with relativistic modifications, in which the mass-velocity and Darwin corrections are included within modified differential equations [26]. Our IC DR program then determines the quantum defects and quadrupole parameters for high values of ℓ by either extrapolation of the relativistic Hartree-Fock (HF) values or from perturbation theory using hydrogenic wave functions; the code is set to choose the maximum value for each of the two quantities calculated by these methods. For values of $\ell\geqslant 8$, we calculate the spin-orbit parameter of the outer electron using a hydrogenic formula and ignore the exchange parameters.

In the case of Si^{11+}, the maximum values for all the quadrupole parameters and quantum defects are those determined by extrapolation of the relativistic HF values. The extrapolated relativistic HF values are different from those calculated from hydrogenic wave functions in this eleven-times ionized species mainly because of the of the mass-velocity correction, the effects of which are included in our relativistic HF wave functions, but only perturbatively in our calculations using hydrogenic wavefunctions. The dashed curve and the solid circles represent the results of our electric-field-mixed and crossed-fields-mixed calculations for this choice of quantum defects and quadrupole parameters. However, for comparison, we also show the results of these same calculations when perturbation theory and hydrogenic wave functions are used to determine the quantum defects and quadrupole parameters for high values of ℓ. The dot-dashed curve and open triangles represent the results of these calculations. As we see, this change in atomic structure

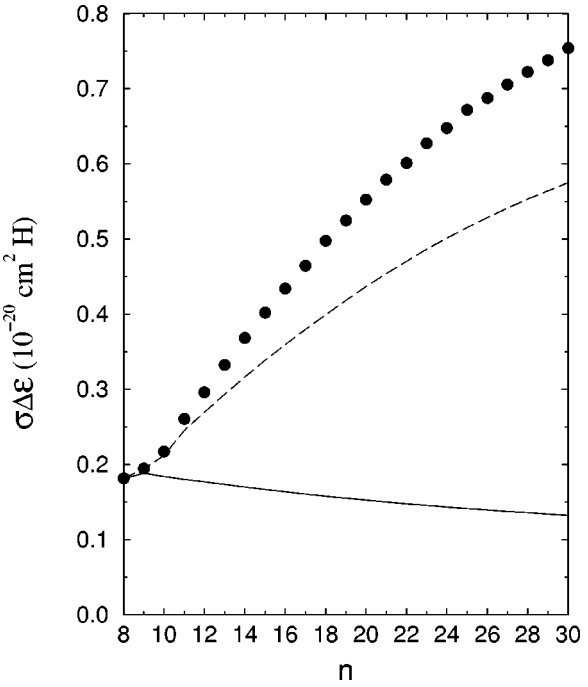

FIG. 4. The energy-averaged dielectronic recombination cross section times the energy-bin width as a function of n for C^{3+} from a CA calculation. Solid curve, no fields; dashed curve, an electric field of 12 V/cm, but no magnetic field; solid circles, an electric field of 12 V/cm and a magnetic field of 24 G.

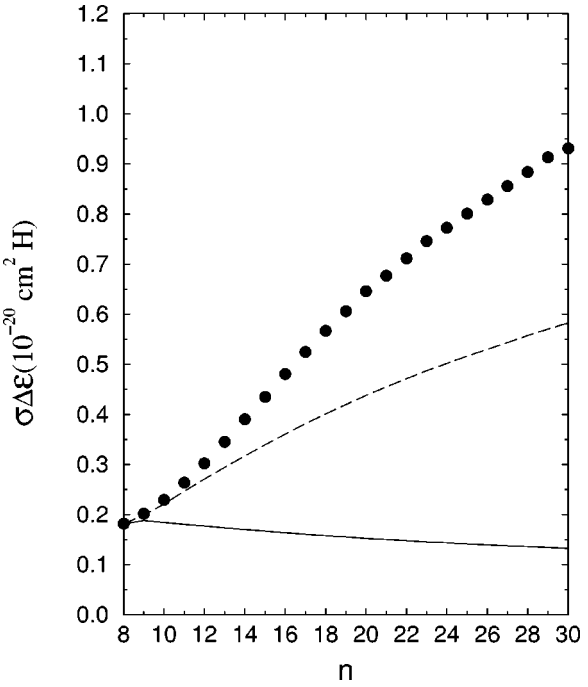

FIG. 5. The energy-averaged dielectronic recombination cross section times the energy-bin width as a function of n for C^{3+} from a CA calculation. Solid curve, no fields; dashed curve, an electric field of 30 V/cm, but no magnetic field; solid circles, an electric field of 30 V/cm and a magnetic field of 180 G.

has only a small effect on the electric-field-mixed results, but begins to have a sizable effect on our results in the presence of crossed electric and magnetic fields for $n \geq 26$. In this case, we believe that the quantum defects and quadrupole parameters determined from extrapolation of the relativistic HF values are the most accurate. However, this sensitivity of the theoretical crossed-fields DR cross sections to the atomic structure of the high-ℓ Rydberg states makes it difficult to estimate the accuracy of the theoretical calculations.

We now consider the results of our CA calculations on C^{3+} and Si^{11+}. In Fig. 4, we present the CA values of $\sigma\Delta\epsilon$ for C^{3+} from $n=8$ to $n=30$, for no fields, an electric field of 12 V/cm and no magnetic field, and finally an electric field of 12 V/cm and a magnetic field of 24 G. Comparing this with the results of the IC calculation in Fig. 1, we see that the CA values are much larger for the lower values of n than are the IC results. By $n=30$, the CA values of $\sigma\Delta\epsilon$ in the presence of the electric field alone are still about 40% higher than the IC values, but the crossed-fields results from the two calculations are closer.

In Fig. 5, we present our CA results for C^{3+} from $n=8$ to $n=30$, with no fields, an electric field of 30 V/cm and no magnetic field, and an electric field of 30 V/cm and a magnetic field of 180 G; this should be compared to the results from our IC calculations in Fig. 2. The situation here is similar to that shown in Fig. 4, except that the enhancement of DR due to the electric field alone is only slightly larger, while the added enhancement arising from the crossed fields shows a noticeable increase. Again the CA field-mixed results yield a larger field enhancement for relatively low values of n; however, in this case, the IC crossed-fields results are actually 15% higher than the corresponding CA values at $n=30$. This may indicate that the crossed-fields enhancement is overestimated by the IC calculation, possibly due to an underestimate of the separation between levels for high values of ℓ.

Finally in Fig. 6, we show our CA results for Si^{11+} for $n=14$ to $n=30$, with no field, an electric field of 100 V/cm and no magnetic field, and an electric field of 100 V/cm and a magnetic field of 300 G; this should be compared to the results of our IC calculation in Fig. 3. Here we see that the CA calculation yields DR cross sections, with or without fields, which are significantly above their IC counterparts. As discussed, in, Griffin, Pindzola, and Bottcher [24], even in the absence of an external field, the CA approximation is only valid when the autoionizing rates are much larger than the radiative rates, or vice versa, for all levels of a given configuration. This condition does not seem to hold in the case of Si^{11+}. Furthermore, as we have seen from the IC calculations, the crossed-fields enhancement of DR is sensitive to the separation between the levels within the doubly excited configurations, and this level structure is not included in the CA approximation. On this basis, we might expect that the CA calculations would significantly overestimate the DR cross section when compared to experiment.

B. Comparisons with experiment

Although it is not possible at the present time to carry out IC calculations of DR in the presence of crossed electric and magnetic fields to high enough values of n to enable comparisons with total DR measurements, this can be done in the case of the CA approximation. In Fig. 7(a), we show such a comparison with the earlier measurements of Dittner *et al.* [13]. As indicated before, the electric field of 30 V/cm and a

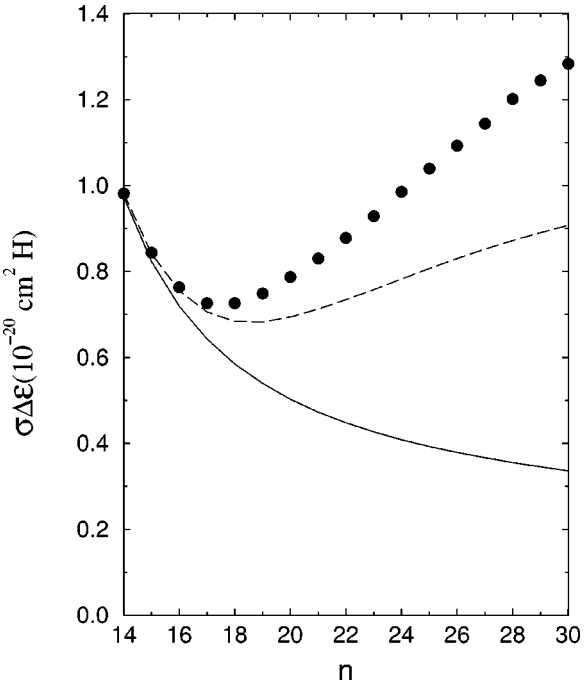

FIG. 6. The energy-averaged dielectronic recombination cross section times the energy-bin width as a function of n for Si^{11+} from a CA calculation. Solid curve, no fields; dashed curve, an electric field of 100 V/cm, but no magnetic field; solid circles, an electric field of 100 V/cm and a magnetic field of 300 G.

crossed magnetic field of 180 G were chosen to match the experimental conditions of this measurement.

These experiments do not measure the DR cross section, but rather a rate coefficient as a function of energy that includes the effects of a small component of the electron velocity perpendicular to the ion beam, with a highly asymmetric distribution; and a component of the velocity parallel to the ion beam, with a symmetric distribution. As can be seen from this figure, these early DR experiments had an electron distribution that was far too wide to resolve resonances associated with individual n values. It is somewhat satisfying that the experimental values are, in general, between the CA results in the presence of the electric field alone and those in the presence of the crossed electric and magnetic fields. In order to provide some indication of what might result from an IC calculation for the crossed-fields case, we also show a comparison of the IC calculation with no field and an electric field of 30 V/cm with the same experimental points in Fig. 7(b). It is hard to say whether the IC calculation for the crossed-fields case would go through the experimental points, but a comparison between the solid circles in Figs. 2 and 5 would indicate that it might be close, but perhaps somewhat high.

In Fig. 8(a), we show a similar comparison of the CA calculation for Si^{11+} with the experimental measurements of Bartsch *et al.* [21] at a field of 91.5 V/cm and a crossed magnetic field of 300 G. Here the electron-distribution is quite narrow and the experiment is close to the point of resolving some of the resonances associated with individual values of n, even for the relatively high values of n in this energy region. As we might expect from the discussion above, the CA calculation yields results for the rate coefficient that are far too large compared to experiment. This is not only due to the breakdown of the approximation itself, but also because the CA approximation does not separate the $2p_{1/2}n\ell$ resonances from the $2p_{3/2}n\ell$ resonances. In Fig. 8(b) we show the no field and electric-field-mixed IC results

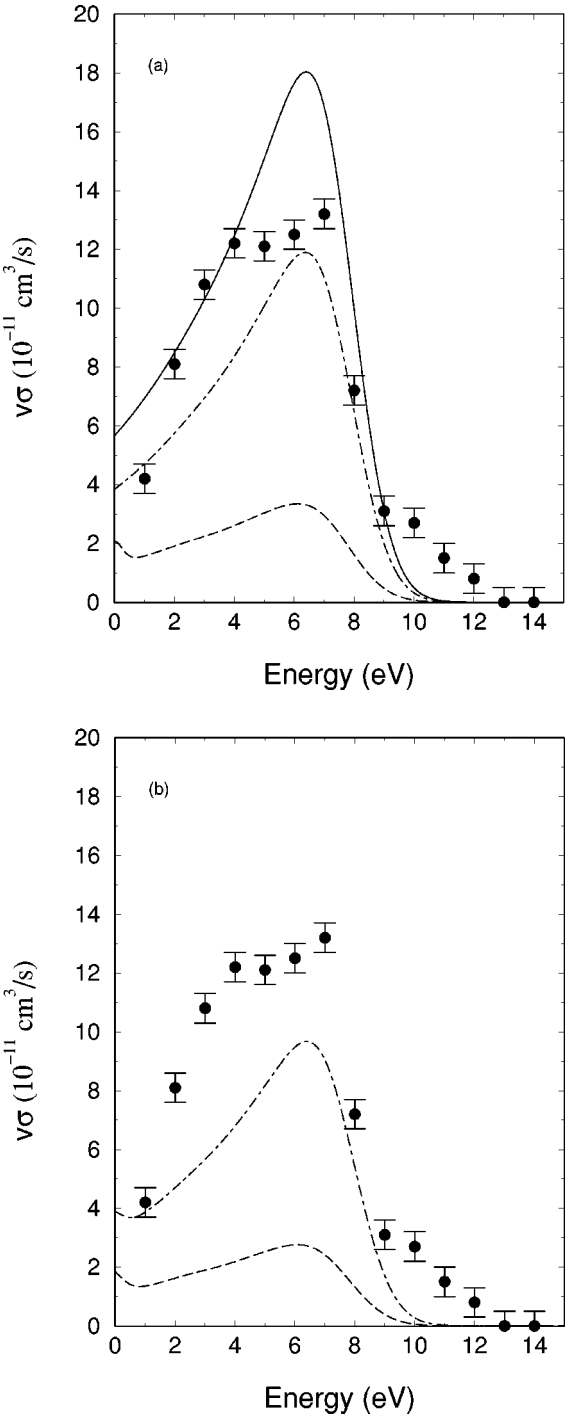

FIG. 7. Dielectronic recombination rate coefficients for C^{3+} (a) From a CA calculation for no fields (dashed curve), an electric field of 30 V/cm and no magnetic field (dashed-dot curve), and an electric field of 30 V/cm and a magnetic field of 180 G (solid curve). (b) From an IC calculation for no fields (dashed curve), and an electric field of 30 V/cm and no magnetic field (dashed-dot curve). The maximum value of n included in both sets of calculations is 44. The experimental points are from Ref. [13] for an approximate electric field of 30 V/cm and a crossed magnetic field of 180 G.

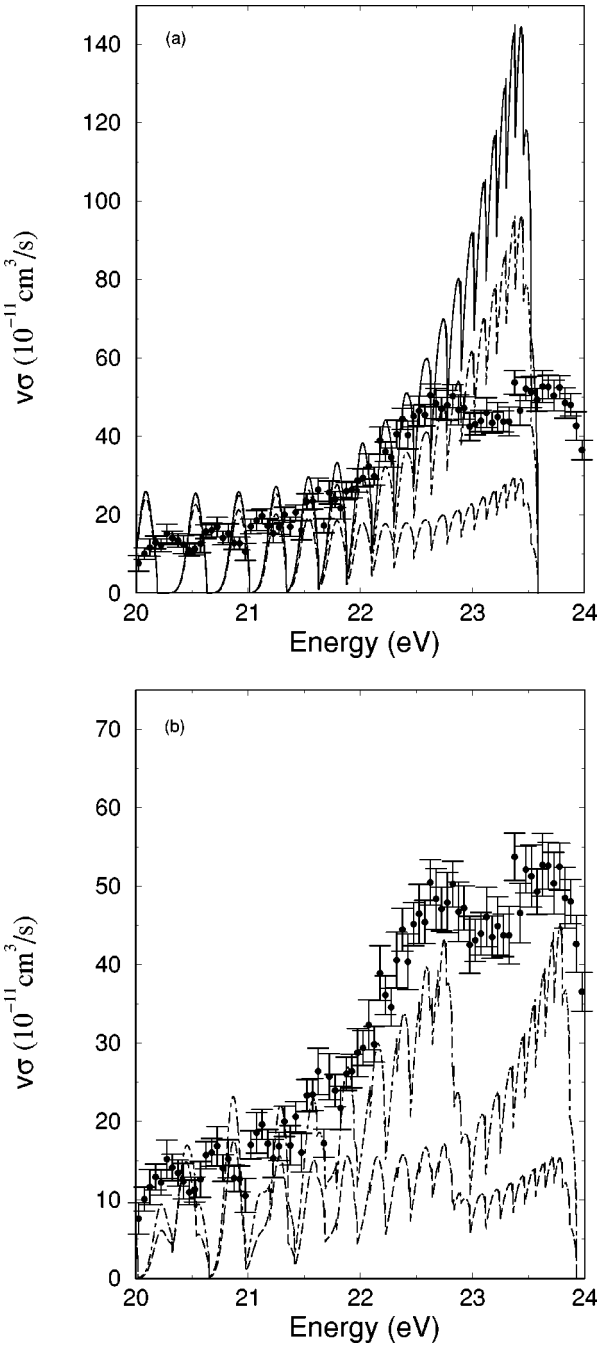

FIG. 8. Dielectronic recombination rate coefficients for Si^{11+}. (a) From a CA calculation for no fields (dashed curve), an electric field of 91.5 V/cm and no magnetic field (dashed-dot curve), and an electric field of 91.5 V/cm and a magnetic field of 300 G (solid curve). (b) From an IC calculation for no fields (dashed curve) and an electric field of 91.5 V/cm and no magnetic field (dashed-dot curve). In both sets of calculations, the maximum values of n is 38. The experimental points are from Ref. [21] for an electric field of 91.5 V/cm and a crossed magnetic field of 300 G.

in comparison to the experimental points. There is some indication that the separation between the $2p_{1/2}n\ell$ and $2p_{3/2}n\ell$ resonances is smaller experimentally than that predicted from the theory, which results in the larger dip at 23 eV in the calculated rate coefficient. This is somewhat surprising because we made a small adjustment in the theoretical spin-orbit parameter for the 2 p electron to make it agree with the experimental separation between $2p_{1/2}$ and $2p_{3/2}$ levels in Si^{11+}. Nevertheless, a comparison of the solid circles with the dashed line in Fig. 3 would indicate that an IC calculation might result in reasonable agreement with the experimental measurements, although again, it may be somewhat high.

C. Partial field-mixed DR for individual values of n

Even if we could carry out our IC calculations for DR in the presence of crossed electric and magnetic fields to values of n comparable to the maximum values of n in the various experimental measurements of total DR, comparisons with the experiment would still present serious difficulties. In all of these experiments, the ions travel from the interaction region, where recombination in the presence of the crossed electric and magnetic fields occurs, to the analyzing region, where the Rydberg states with high values of n are field ionized in a very large Lorentz field. As these field-mixed, recombined ions travel toward the detector, the high-n Rydberg states have time to radiatively decay to lower values of n, thus introducing an uncertainty regarding how many of these states will survive the stripping field. Even without this uncertainty, the calculation of field ionization of field-mixed Rydberg states for nonhydrogenic systems presents a significant challenge. Thus, one of the most serious difficulties in making comparisons with total DR experiments is the determination of what values n should be included in the theoretical calculations.

A solution to this problem would be to study field effects in a set of recombination resonances associated with a particular intermediate value of n that is small enough to survive the stripping field, but large enough to show significant field-mixing effects. However, until now, the resolution of these experiments has been insufficient to separate the resonances associated with different intermediate values of n. That now appears to be changing. Recently Zong *et al.* [27] reported on high resolution measurements of DR in Li-like argon in which they resolved, separately, the groups of resonances from $2p_{1/2}n\ell$ and $2p_{3/2}n\ell$ for a given value of n up to $n=18$, and with the help of calculations, up to $n=23$.

For this reason, we have calculated values of $\sigma\Delta\epsilon$ for both the $2p_{1/2}24\ell$ and $2p_{3/2}24\ell$ resonances with no magnetic field and with a magnetic field of 300 G and the eight values of the electric-field strengths employed in the experiment of Bartsch *et al.* [21]. The results are presented in Table I. We chose $n=24$, since it is high enough to show significant field enhancement, yet small enough to easily survive the stripping field and have a chance of being resolved from adjacent n values. In the last three columns of this table, we give the ratio of the value of $\sigma\Delta\epsilon$ calculated in the presence of crossed electric and magnetic fields to the value of $\sigma\Delta\epsilon$ calculated with only the electric field. This provides a measure of the added enhancement due to the crossed magnetic field. In Fig. 9, we present calculated field-enhancement ratios for $n = 24$, with an electric field only and with crossed electric and magnetic fields; these are simply the ratios of the field-mixed values of $\sigma\Delta\epsilon$ to their values with no fields present.

From Table I and Fig. 9, we notice that the field enhancement of the DR cross section is significantly larger for the

TABLE I. DR cross section times the energy-bin width for Si^{11+} with $n=24$ as a function of electric-field strength E, with $B=300$ G.

Energy ($j_j=1/2$)=0.775805 H				Energy ($j_j=3/2$)=0.814037 H					
	$\sigma\Delta\epsilon$ (E only) (10^{-20} cm^2 H)			$\sigma\Delta\epsilon$ ($E\times B$) (10^{-20} cm^2 H)			Ratio for added enhancement from the crossed magnetic field		
E (V/cm)	$j_j=1/2$	$j_j=3/2$	total	$j_j=1/2$	$j_j=3/2$	total	$j_j=1/2$	$j_j=3/2$	total
0.0	0.1109	0.2244	0.3353	0.1109	0.2244	0.3353	1.000	1.000	1.000
9.2	0.1331	.2291	0.3622	0.1411	0.2465	0.3876	1.060	1.076	1.070
18.4	0.1463	0.2377	0.3840	0.1559	0.2741	0.4300	1.066	1.153	1.119
32.0	0.1670	0.2534	0.4204	0.1815	0.3116	0.4931	1.087	1.230	1.173
46.0	0.1854	0.2697	0.4551	0.2108	0.3379	0.5487	1.137	1.253	1.206
68.8	0.2065	0.2938	0.5002	0.2495	0.3660	0.6155	1.208	1.246	1.231
91.5	0.2208	0.3117	0.5324	0.2829	0.3853	0.6682	1.281	1.236	1.255
137.5	0.2392	0.3391	0.5784	0.3273	0.4192	0.7465	1.368	1.236	1.291
183.1	0.2517	0.3605	0.6121	0.3509	0.4464	0.7973	1.394	1.238	1.303

$j_j=1/2$ resonances than for the $j_j=3/2$ resonances in the presence of the electric field alone, and especially with the crossed electric and magnetic fields. Furthermore, the enhancement of the $2p_{1/2}n\ell$ resonances in crossed electric and magnetic fields is increasing at a much higher rate than is the case for the $2p_{3/2}n\ell$ resonances. This is due to the difference in structure between the $j_j=1/2$ and the $j_j=3/2$ levels. As mentioned earlier, the quadrupole Slater parameter $F^2(2pn\ell)$ only affects the structure of the $2p_{3/2}n\ell$ levels, and as ℓ becomes large this is the only factor, other than the quantum defect, that has any appreciable effect on their energies. Thus, the four levels for a given $2p_{1/2}n\ell$ subconfiguration become degenerate for high ℓ and the mixing effects between magnetic states within the subconfiguration become large. This again points to the sensitivity of DR cross sections in the presence of crossed electric and magnetic fields to the details of the level structure of the high-ℓ Rydberg states.

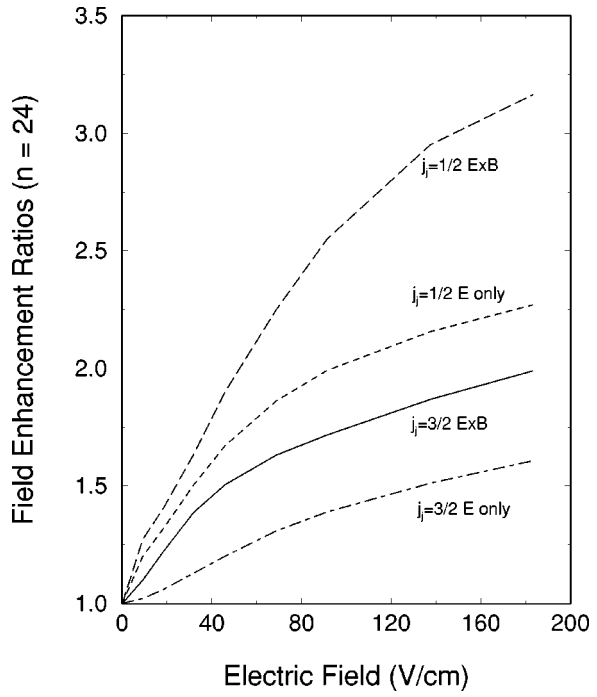

FIG. 9. Plot of the enhancement of the zero-field DR cross section of the $2p_{1/2}24\ell$ and $2p_{3/2}24\ell$ resonances in Si^{11} by an electric field (short-dashed and dot-dashed curves) and by an electric-field crossed with a magnetic field of 300 G (long-dashed and solid curves) as a function of electric-field strength.

IV. CONCLUSIONS

The results presented in this paper support the predictions made by Robicheaux and Pindzola [22] regarding the additional enhancement of dielectronic recombination provided by the presence of a magnetic field crossed with an electric field. Our comparisons of DR cross sections as a function n demonstrate the importance of the energy-level structure of high Rydberg states to the calculation of field-mixed DR. The CA approximation tends to overestimate the size of the field-mixed cross section, especially for lower values of n and lower field strengths. This is supported by our comparisons of the CA results with measurements of total DR.

Experimental measurements are now reaching sufficient resolution that it may soon be possible to study field effects on a group of resonances associated with a given value of n, by comparison of experiment with calculations such as the one presented here for $n=24$. This would eliminate the primary difficulty in making comparisons between theory and experiment for the total field-mixed DR; namely, the uncertainty regarding the maximum value of n to be included in the theoretical calculations.

Although experimental studies of field-mixed partial DR cross sections would eliminate the necessity of pushing the IC calculations to high values of n, we are now beginning to investigate computational methods that may make it possible to carry these calculations to higher n values, and at the same time, improve their accuracy. We are considering modifying the present code to solve this intermediate-coupled field-mixed problem using techiques that will only require us to store the nonzero elements of the Hamiltonian matrix, and which can be implemented on a massively parallel machine. Furthermore, we are hoping that it may be possible to include the higher-order effects associated with overlapping, interacting resonances. The inclusion of these effects, coupled with some improvements in the calculation of the structure of the high-ℓ resonances, may also remove some of

the uncertainty associated with the accuracy of the present IC calculations.

V. ACKNOWLEDGMENTS

The authors wish to thank Alfred Müller for providing them with experimental data on DR in Si^{11+} before publication and Ken LaGattuta for sending the preprint of his paper on field effects in Mg^{+}. This work was supported by the U. S. Department of Energy, Office of Fusion Energy, under Contract No. DE-FG05-93ER54218 with Rollins College and Contract No. DE-FG05-86ER53217 with Auburn University and a DOE EPSCOR Grant DE-FC02-91ER75678 with Auburn University.

[1] A. Burgess and H. P. Summers, Astrophys. J. **157**, 1007 (1969).
[2] V. L. Jacobs, J. Davis, and P. C. Kepple, Phys. Rev. Lett. **37**, 1390 (1976).
[3] V. L. Jacobs and J. Davis, Phys. Rev. A **19**, 776 (1979).
[4] W. Huber and C. Bottcher, J. Phys. B **13**, L399 (1980).
[5] K. LaGattuta and Y. Hahn, Phys. Rev. Lett. **51**, 558 (1983).
[6] K. LaGattuta, J. Phys. B **18**, L467 (1985).
[7] K. LaGattuta, I. Nasser, and Y. Hahn, Phys. Rev. A **33**, 2782 (1986).
[8] D. C. Griffin, M. S. Pindzola, and C. Bottcher, Phys. Rev. A **33**, 3124 (1986).
[9] C. Bottcher, D. C. Griffin, and M. S. Pindzola, Phys. Rev. A **34**, 860 (1986).
[10] D. C. Griffin and M. S. Pindzola, Phys. Rev. A **35**, 2821 (1987).
[11] D. C. Griffin, M. S. Pindzola, and P. G. Krylstedt, Phys. Rev. A **40**, 6699 (1989).
[12] P. F. Dittner, S. Datz, P. D. Miller, P. L. Pepmiller, and C. M. Fou, Phys. Rev. A **33**, 124 (1986).
[13] P. F. Dittner, S. Datz, P. D. Miller, P. L. Pepmiller, and C. M. Fou, Phys. Rev. A **35**, 3668 (1987).
[14] P. F. Dittner, S. Datz, H. F. Krause, P. D. Miller, P. L. Pepmiller, C. Bottcher, C. M. Fou, D. C. Griffin, and M. S. Pindzola, Phys. Rev. A **36**, 33 (1987).
[15] P. F. Dittner, S. Datz, R. Hippler, H. F. Krause, P. D. Miller, P. L. Pepmiller, C. M. Fou, Y. Hahn, and I. Nasser, Phys. Rev. A **38**, 2762 (1988).
[16] A. Müller, D. S. Belic, B. D. DePaola, N. Djurić, G. H. Dunn, D. W. Mueller, and C. Timmer, Phys. Rev. Lett. **56**, 127 (1986).
[17] L. H. Andersen, J. Bolko, and P. Kvistgaard, Phys. Rev. A **41**, 1293 (1990).
[18] L. H. Andersen, G. Y. Pan, H. T. Schmidt, M. S. Pindzola, and N. R. Badnell, Phys. Rev. A **45**, 6332 (1992).
[19] A. R. Young, L. D. Gardner, D. W. Savin, G. P. Lafyatis, A. Chutjian, S. Bliman, and J. L. Kohl, Phys. Rev. A **49**, 357 (1994).
[20] D. W. Savin, L. D. Gardner, D. B. Reisenfeld, A. R. Young, and J. L. Kohl, Phys. Rev. A **53**, 280 (1996).
[21] T. Bartsch, A. Müller, W. Spies, J. Linkemann, H. Danared, D. R. DeWitt, H. Gao, W. Zong, R. Schuch, A. Wolf, G. H. Dunn, M. S. Pindzola, and D. C. Griffin, Phys. Rev. Lett. **79**, 2233 (1997).
[22] F. Robicheaux and M. S. Pindzola, Phys. Rev. Lett. **79**, 2237 (1997).
[23] K. LaGattuta (private communication).
[24] D. C. Griffin, M. S. Pindzola, and C. Bottcher, Phys. Rev. A **31**, 568 (1985).
[25] R. D. Cowan, *The Theory of Atomic Structure and Spectra* (University of California, Berkeley, 1981).
[26] R. D. Cowan and D. C. Griffin, J. Opt. Soc. Am. **66**, 1010 (1976).
[27] W. Zong, R. Schuch, E. Lindroth, H. Gao, D. R. DeWitt, S. Asp, and H. Danared, Phys. Rev. A **56**, 386 (1997).